DOI: 10.1002/chem.201001287

A Micelle-Based Chemosensing Ensemble for the Fluorimetric Detection of Chloride in Water

Thomas Riis-Johannessen and Kay Severin*[a]

Optical chemosensors respond to target analytes by simple changes in absorbance or fluorescence emission. They are powerful analytical tools that require little in the way of specialist equipment (a UV/Vis or fluorescence spectrometer) and can be reliably implemented by the nonexpert for sensing a wide range of analytes.[1]

The classical design entails covalently linking a receptor with a chromo- or fluorophore to yield a conjugate chemosensor. The binding site and spectroscopic handle can be tuned to yield optimal signal output and selectivity, but often only at the expense of considerable synthetic effort. This latter concern has, in part, stimulated the development of an alternative approach wherein the receptor and signaling units are physically distinct entities that interact through supramolecular interactions.[2] These types of sensors are referred to as chemosensing ensembles and they come in different guises. A particularly successful variant is the indicator displacement assay (IDA), in which a dye competes with the analyte for binding to a synthetic receptor.[3] Another type of chemosensing ensemble relies on micelles to preassemble a receptor and signaling unit.[4,5] By analogy with the conjugate chemosensor, an amphiphilic receptor and a hydrophobic fluorophore are confined within the nanosized volume of a micelle. When bound to the receptor, the proximity of the analyte to the signaling unit then results in fluorescence quenching, enabling optical detection of the analyte (Figure 1a).

This self-assembly strategy can be optimized by using simple combinatorial procedures[4] and has now been applied for sensing a range of transition-metal cations.[4,5] However, it is only applicable to analytes that are able to quench the micelle-encapsulated fluorophore (by, e.g., electron transfer or heavy atom effects). Herein, we describe a conceptually different approach for the construction of a micelle-based chemosensing ensemble. The components include a commercially available fluorophore and surfactant, and an easy-to-prepare rhodium(III)-based receptor. In our system, however, it is the receptor that functions as a quencher, and its presence within the micelle is provoked by a favorable change in the partition coefficient; this occurs on binding of the analyte (Figure 1b). The micelle dispersion thus provides both a secondary pseudo phase in which the receptor–chloride complex is selectively stabilized and a platform on which to juxtapose the receptor and reporter subunits for signal transduction.

For our study we have chosen a simple but challenging target analytical: the chloride ion. Chloride plays crucial roles in a number of biological and environmental processes and is strongly implicated in certain medical conditions.[6a]

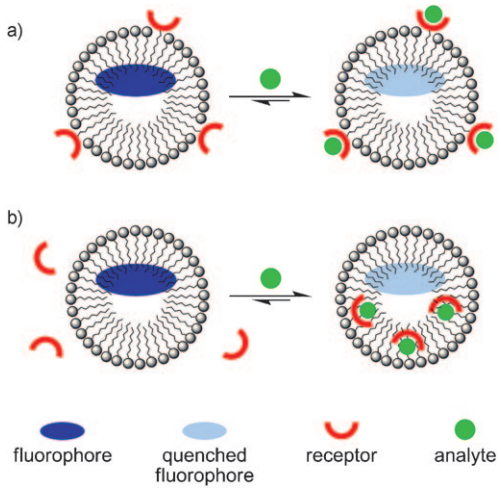

Figure 1. Micelle-based sensing ensembles. a) Template-assisted assembly of a receptor and fluorophore within a micelle: binding of the analyte to the receptor leads to fluorescence attenuation only for analytes which can quench the fluorophore. b) Phase transfer of a receptor–analyte complex from the bulk to a fluorophore-doped micellar phase: fluorescence attenuation requires only that the receptor can quench the fluorophore.

[a] Dr. T. Riis-Johannessen, Prof. K. Severin
Institut des Sciences et Ingénierie Chimiques
Ecole Polytechnique Fédérale de Lausanne (EPFL)
1015 Lausanne (Switzerland)
Fax: (+41) 21-693-9305
E-mail: kay.severin@epfl.ch

Supporting information for this article is available on the WWW under http://dx.doi.org/10.1002/chem.201001287.

The literature features numerous compounds that respond selectively to chloride through an optical signal. One class relies on nonspecific transient interactions between an excited-state fluorophore and chloride, which quenches the emission of the former (i.e., dynamic quenching).[6] These systems are suited for sensing in the millimolar range, but they lack the sensitivity for lower concentrations. Receptor-based chemosensors, on the other hand, typically exploit multiple noncovalent hydrogen-bonding or electrostatic interactions for chloride recognition, and they generally function well in nonaqueous media.[7] However, chloride sensing is most relevant in water, in which its affinity for a given receptor can be dramatically diminished due to persistent solvation.[8] Consequently, systems capable of binding and signaling chloride in homogenous aqueous/organic media remain few,[9] whereas those that can achieve this in pure water are fewer still.[10] The micelle-based chemosensing ensemble described below allows sensing of chloride in buffered aqueous solution with a selectivity and sensitivity that is unprecedented for receptor-based chemosensors.

Our choice of receptor was inspired by reports from the context of medicinal chemistry that complexes of the type $[Ru(\eta^6\text{-arene})(en)(H_2O)]^{2+}$ (en = ethylenediamine) can coordinate Cl^- in water with $\log K$ values of up to 2.1.[11] We therefore decided to explore whether half-sandwich complexes could be used for sensing chloride in water. Instead of (η^6-arene)Ru^{II} complexes, we used a Cp^*Rh^{III} complex (**1a**, $Cp^* = C_5Me_5$; Scheme 1), which tends to be more robust toward oxidation.[12]

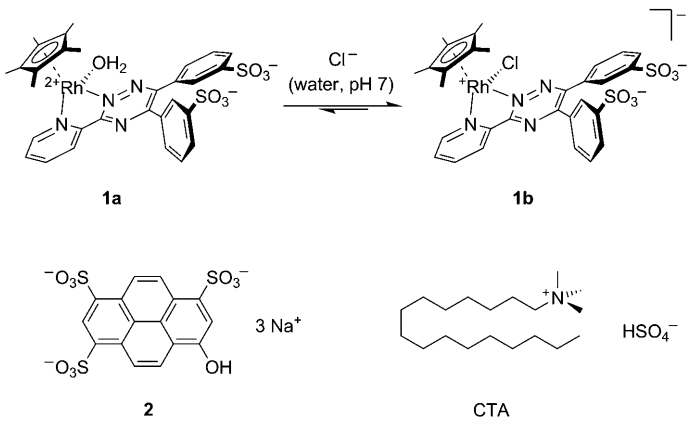

Scheme 1. Components of the chemosensing ensemble: aqua complex **1a**, chloro-adduct **1b**, fluorophore **2**, and cationic surfactant CTA.

Receptor **1a** is prepared in situ by simply combining two equivalents of commercially available Ferrozine (Fz) ligand[13] with the hydroxy-bridged rhodium(III) dimer $[Rh(Cp^*)_2(\mu\text{-}OH)_3][NO_3]$[14] in buffered MOPS (MOPS = 3-(4-morpholinyl)-1-propanesulfonic acid) solution (50 mM, pH 7.0). ESIMS shows intense peaks for ions $[\mathbf{1a}-H]^-$ (*m*/*z* −705.38), $[\mathbf{1a}+H]^+$ (*m*/*z* 707.11), $[\mathbf{1a}+Na]^+$ (*m*/*z* 729.13), $[\mathbf{1a}+2H]^{2+}$ (*m*/*z* 354.03), and aqua adducts $[\mathbf{1a}+H_2O+H+Na]^{2+}$ (*m*/*z* 374.55) and $[\mathbf{1a}+H_2O+2Na]^{2+}$ (*m*/*z* 385.54), while UV/Vis titrations confirm quantitative formation under the specified conditions ($\log K \geq 8.2$, Figure S1 in the Supporting Information). ^1H NMR spectroscopy studies reveal a pronounced chemical shift dependence on pH (7–10) for the proton adjacent to the pyridyl nitrogen, which is attributed to deprotonation of a nearby rhodium(III)-bound aqua ligand (Figure S2 in the Supporting Information). By using the Henderson–Hasselbach equation, a pK_a of 8.34(5) was calculated for the latter. At pH 7.0, therefore, compound **1a** exists in solution as a neutral zwitterionic aqua complex (Scheme 1).

Addition of NaCl to **1a** causes smooth variations in absorbance (Figure S3 in the Supporting Information) that fit to a 1:1 binding isotherm with $\log K = 2.82(5)$. Formation of the chloro-adduct $[Rh(Cp^*)Cl(Fz)]^-$ (**1b**) is also accompanied by the appearance of a peak for $[\mathbf{1b}]^-$ (*m*/*z* −741.10) in the ESIMS spectrum, and a new set of aromatic resonances in the ^1H NMR spectrum (Figure S4 in the Supporting Information). The anation constant is higher than those reported for ruthenium(II) half-sandwich complexes.[11] Indeed, it is comparable with those obtained for much more elaborate receptors,[6,15] despite the former relying on the formation of only one metal–ligand coordinative interaction. The implications for chloride sensing in water are thus promising. Nevertheless, two factors limit the scope of **1a** in terms of optical sensing: 1) the absorption spectra of **1a** and **1b** are too similar for a direct colorimetric readout, and 2) with $\log K = 2.82(5)$, a high concentration of **1a** would be essential for achieving detection limits below the millimolar range.

In principle, these issues could be addressed by synthetic design. The *N,N*-chelate or π ligand in **1a** could be modified to increase the Lewis acidity, and hence chloride affinity, of the metal center. Likewise, signal amplification could be achieved by, for example, appending an optical reporter fragment to one or other of the two ligands. To avoid tedious chemical manipulations, however, we opted to explore a supramolecular approach based on the use of receptor/dye interactions in self-assembled surfactant micelles.

Micelles constitute a pseudo-secondary phase, the core and interfacial regions of which offer unique microenvironments. Partitioning inside a micelle can dramatically alter the physio-chemical properties of a molecule. Consequently, the influence of surfactants on reaction kinetics and thermodynamics has long been an active area of research.[16] Since the binding of chloride to **1a** reduces the net positive charge associated with the Cp^*Rh^{III} fragment, chloro-adduct **1b** may be considered as more amphiphilic than its aqua precursor. A suitable surfactant additive could therefore provide a dispersed phase into which **1b** is selectively stabilized. The implied phase-transfer phenomenon would also constitute an indirect means of enhancing the chloride affinity of **1a**.

We found that cetyltrimethylammonium (CTA) hydrogensulfate had the desired effect on the chloride binding affinity of **1a**. Under working conditions ($[\mathbf{1a}]_{tot} = 500$ μM, 50 mM MOPS, pH 7.0), surface tension measurements indicate a critical micelle concentration (*cmc*) of approximately 30 μM

(Figure S5 in the Supporting Information), which compares well with that reported for CTA in the presence of 50 mM Na_2SO_4.[17] UV/Vis titrations of Cl^- into solutions of **1a** (500 μM) in MOPS buffer (50 mM, pH 7.0) were then performed with increasing amounts of CTA present and apparent stability constants, K_{app}, were determined (Figure S3 in the Supporting Information). A plot of $\log K_{app}$ versus [CTA] is shown in Figure 2. As can be seen, K_{app} increases by two orders of magnitude before starting to level off above [CTA] ≈ 20 mM.

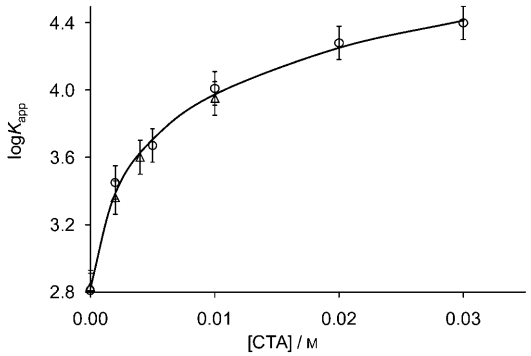

Figure 2. Changes in $\log K_{app}$ for binding of Cl^- by **1a** with increasing surfactant concentration ($[CTA]_{tot}$ = 0–30 mM, 50 mM MOPS, pH 7.0). Data for two series of titrations, one with $[\mathbf{1a}]_{tot}$ = 500 μM (○) and one with $[\mathbf{1a}]_{tot}$ = 100 μM (△) are shown. The line is calculated from Equation (1) by using best fit parameters discussed in the main text.

Within experimental error, the same trend occurs for a series of titrations with $[\mathbf{1a}]_{tot}$ = 100 μM. Both data sets were thus fitted simultaneously to Equation (1), which relates the observed variation in K_{app} with R [the relative micellar volume; $R = ([CTA]_{tot} - cmc)V_\phi$, in which $V_\phi = 0.361\ M^{-1}$ is the partial molar volume of micellized surfactant][18] to an intrinsic binding constant K (in the absence of micelles) and partition constants, $K_{p,\mathbf{1a}}$ and $K_{p,\mathbf{1b}}$, describing the distribution of **1a** and **1b**, respectively, in the water/micelle biphase.

$$K_{app} = K[(1-R+K_{p,\mathbf{1b}}R)/(1-R)(1-R+K_{p,\mathbf{1a}}R)] \quad (1)$$

With K fixed at $10^{2.82} = 660\ M^{-1}$, best fits were obtained when $K_{p,\mathbf{1a}} = 7 \pm 2$ and $K_{p,\mathbf{1b}} = 3700 \pm 500$. The marked increase in K_{app} as CTA is added is thus due to the pronounced tendency of **1b** to partition within the micelle pseudo phase: that is, the micelle/water partition constant of the receptor increases by three orders of magnitude on binding Cl^-. Parallel UV/Vis titrations of CTA into solutions of **1a** (500 μM), with and without $[Cl]_{tot}$ = 30.0 mM present, ratify these observations. Only under conditions in which **1b** is the majority species do the spectra evolve to any great extent when CTA is added (Figure S6 in the Supporting Information) and fitting these changes to a two-phase partition model[19] gives a comparable value of $K_{p,\mathbf{1b}} = 2000 \pm 400$. Similar phenomena are also observed by ^1H NMR spectroscopy (Figure S7 in the Supporting Information).

Next, we focused our attention on developing a signal transduction mechanism to report on the binding and phase-transfer events associated with the interaction between **1a** and Cl^- in the water/micelle dispersion. To this end, we introduced fluorescent dye 8-hydroxypyrene-1,3,6-trisulfonate (**2**, Scheme 1). In aqueous CTA solution, with $[CTA]_{tot} > cmc$, compound **2** also partitions within the micelle pseudo phase.[20] This causes a shift in emission maximum, λ_{em}, from 510 to 528 nm and increases the ground-state pK_a of its hydroxyl group from 7.4 to ≈10.[21]

The effect of complexes **1a** and **1b** on the emission of **2**, with varying amounts of CTA present, is shown in Figure 3. Quenching occurs to various degrees in all cases. Particularly noteworthy, however, is the contrast between quenching efficiency of **1a** and **1b** when $[CTA]_{tot}$ = 2.0 mM. The Stern–Volmer plot for **1a** shows only a modest quenching effect, whereas **1b** reduces the fluorescence emission intensity, I_F, by up to 90% at concentrations as low as $[\mathbf{1b}]_{tot}$ = 400 μM. A marked deviation from linearity also occurs for $[\mathbf{1b}]_{tot} \geq$ 100 μM and the data can thus be fitted to a model that takes into account both static and dynamic "sphere-of-action" quenching according to $I_0/I_F = (1+K_s[\mathbf{1b}]_m)e^{(V[\mathbf{1b}]_m)}$, in which $[\mathbf{1b}]_m$ is the concentration of **1b** in the micelle (calculated with $K_{p,\mathbf{1b}}$ = 3700), and K_s and V are the static and dynamic quenching constants, respectively.[22] This gives best-fit values of $K_s = (8430 \pm 300)\ M^{-1}$ and $V = (3900 \pm 200)\ M^{-1}$.

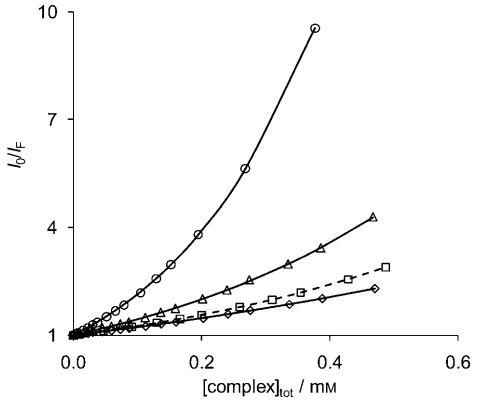

Figure 3. Stern–Volmer plots showing quenching of **2** (12.5 μM) by **1b** in the presence of 2.0 mM (○), 5.0 mM (△), and 10.0 mM (◇) CTA as well as **1a** (□) in the presence of 2.0 mM CTA (50 mM MOPS, pH 7.0). λ_{ex} = 480 nm, λ_{em} = 528 nm.

Fluorescence quenching of **2** has been observed in a number of cases[23] and can proceed by electron transfer from the excited fluorophore to the quencher. The redox properties of the latter can, therefore, strongly affect the efficiency of this process. Indeed, this was explicitly demonstrated for a series of viologen derivatives, the Stern–Volmer quenching constants of which increased markedly with reduction potentials in the range −1000 to −400 mV (vs. NHE).[23a] With values of $E^{\circ\prime} = -325$ and −355 mV (vs. NHE, 50 mM MOPS, pH 7.0), determined by cyclic voltammetry for the one-electron reductions of **1a** and **1b**, respec-

tively (Figure S8 in the Supporting Information), similar donor–acceptor interactions are likely to be responsible for the observed quenching in the present system.

Direct interpretation of the Stern–Volmer parameters derived for **1b** is, however, not straightforward. They reflect both complex association and diffusion phenomena in the micelle pseudo phase[22] and the relative distributions of **1b** and **2** in the colloidal dispersion.[24] The extent to which the relative distributions influences the quenching process can be seen in the curves obtained for $[CTA]_{tot}=5.0$ and 10.0 mM (Figure 3); increasing the surfactant concentration severely dampens the quenching effect. The probability of quencher and fluorophore occupying the same micelle clearly decreases as the micelles increase in number. Consequently, the conditions under which the chloride affinity peaks of **1a** (i.e., $[CTA]_{tot}\geq 20$ mM, see Figure 2) are not those under which the signal transduction is most efficient ($[CTA]_{tot}\approx 2$ mM, see Figure 3).

Such considerations aside, the difference in phase partitioning between **1a** and **1b**, and the implications this has for their respective quenching efficiencies, is still ample for sensing purposes, even with a surfactant concentration as low as $[CTA]_{tot}=2.0$ mM. This is illustrated in Figure 4,

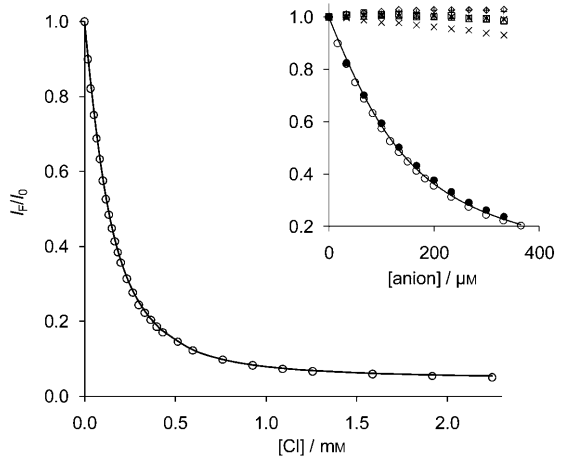

Figure 4. Relative changes in I_F of the chemosensing ensemble described in the text as Cl^- (○) is added. Inset: the observed response for other anions; AcO^- (×), $HP_2O_7^{3-}$ (+), HPO_4^{2-} (*), NO_3^- (□), SO_4^{2-} (◇), HCO_3^- (△) and Cl^- in the presence of all other anions each at 100 μM (●). $\lambda_{ex}=360$ nm, $\lambda_{em}=528$ nm.

which shows the I_F/I_0 response of a solution containing **1a** (500 μM), **2** (12.5 μM), and CTA (2 mM) in MOPS buffer (50 mM, pH 7.0) as Cl^- and various other anions (inset) are added. The chemosensor clearly operates into the low micromolar range and, furthermore, is largely unresponsive to other anions. Acetate provokes a gradual ON–OFF signal, but its relative magnitude in the Cl^- dynamic range is minimal. Pyrophosphate and phosphate, both known to coordinate Cp^*Rh^{III} centers,[25] give no signal at all. The sensor does succumb to the usual interference problems with the heavier halides (Br^- and I^-) and pseudohalide CN^-, presumably due to their superior affinity for direct coordination of the rhodium(III) center in **1a** and related complexes.[26] Such limitations are, however, of little importance given the low concentrations at which these anions typically occur in nature.

To test the practical scope of our sensor, we designed a simple assay for the determination of Cl^- content in drinking water. In a typical experiment, bottled and tap water samples were added to an equal volume of a solution containing **1a** (1.0 mM), **2** (25 μM), and CTA (4.0 mM) in MOPS buffer (100 mM, pH 7.0) to give the same final concentrations (in **1a**, **2**, CTA and MOPS) as those used to obtain the graph depicted in Figure 4. The fluorescence intensities, I_F, of each sample (4–6 repeats) were then measured and compared with a series of 14 blanks, wherein double-distilled water was added. By using the blank readings, a detection limit of approximately 5 μM was determined.[27] The I_F/I_0 values were calculated for each sample and then converted into concentrations by using the data shown in Figure 4 as a calibration curve. A comparison between reported and determined chloride content is presented in Figure 5. As can be seen, the match between the two is excellent for all samples analyzed, an impressive result given that up to five other competing anions (SO_4^{2-}, NO_3^-, SiO_2^{2-}, HCO_3^-, and F^-) are present, some (e.g., HCO_3^-) at concentrations as high as 6 mM.

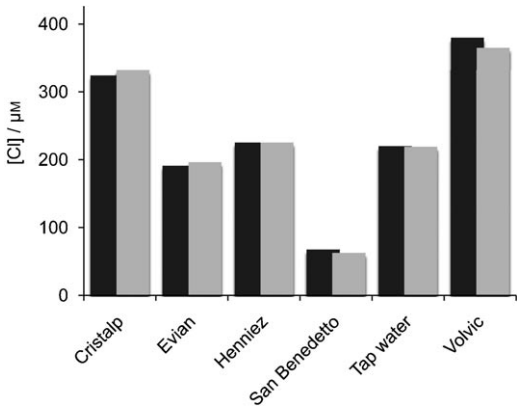

Figure 5. Determined (gray) and reported (black) chloride content of six drinking water samples. The error is ±5 μM.[28]

In summary, we have developed a chemosensing ensemble for the fluorimetric detection of chloride. The system exploits concomitant binding and phase-partitioning events, which confine a receptor-based quencher and a fluorophore to within the small volume of a self-assembled micelle. The presence of micelles also markedly increases the apparent affinity of the receptor for chloride. In principle, the approach can be generalized to any system wherein the association between an analyte and receptor gives rise to a complex with markedly different solvation characteristics. The sensor has a number of other interesting features: 1) it can be made in situ by mixing easily accessible components, 2) it

can be employed in purely aqueous solution at neutral pH, 3) it displays a very high selectivity and sensitivity for chloride, and 4) it employs a novel signal transduction mechanism.

Experimental Section

Complete experimental procedures and details of the fluorimetric assays are given in the Supporting Information.

Acknowledgements

This work was supported by funding from the Swiss National Science Foundation, by the COST action CM0703 on Systems Chemistry, and by the EPFL. We thank Daniel Merki for help with the cyclic voltammetry.

Keywords: analytical methods · chemosensors · fluorescence · micelles · rhodium

[1] U. E. Spichigger-Keller in *Chemical Sensors and Biosensors for Medical and Biological Applications*, Wiley, New York, **2007**.
[2] F. Mancin, E. Rampazzo, P. Tecilla, U. Tonellato, *Chem. Eur. J.* **2006**, *12*, 1844–1854.
[3] B. T. Nguyen, E. V. Anslyn, *Coord. Chem. Rev.* **2006**, *250*, 3118–3127.
[4] P. Grandini, F. Mancin, P. Tecilla, P. Scrimin, U. Tonellato, *Angew. Chem.* **1999**, *111*, 3247–3250; *Angew. Chem. Int. Ed.* **1999**, *38*, 3061–3064.
[5] a) F. Mancin, P. Tecilla, P. Scrimin, U. Tonellato, *Coord. Chem. Rev.* **2009**, *253*, 2150–2165; b) P. Pallavicini, Y. A. Diaz-Fernandez, L. Pasotti, *Coord. Chem. Rev.* **2009**, *253*, 2226–2240.
[6] a) G. D. Geddes, *Meas. Sci. Technol.* **2001**, *12*, R53-R88; b) S. Jayaraman, A. S. Verkman, *Biophys. Chem.* **2000**, *85*, 49–57.
[7] a) P. A. Gale, *Chem. Commun.* **2008**, 4525–4540; b) T. Gunnlaugsson, M. Glynn, G. M. Tocci, P. E. Kruger, F. M. Pfeffer, *Coord. Chem. Rev.* **2006**, *250*, 3094–3117; c) J. W. Steed, *Chem. Commun.* **2006**, 2637–2649; d) P. D. Beer, P. A. Gale, *Angew. Chem.* **2001**, *113*, 502–532; *Angew. Chem. Int. Ed.* **2001**, *40*, 486–516; *Angew. Chem.* **2001**, *113*, 502–532.
[8] J. W. Steed, J. L Atwood in *Supramolecular Chemistry*, Wiley, New York, **2009**.
[9] For selected examples, see: a) A. J. McConnell, C. J. Serpell, A. L. Thompson, D. R. Allen, P. D. Beer, *Chem. Eur. J.* **2010**, *16*, 1256–1264; b) L. M. Hancock, P. D. Beer, *Chem. Eur. J.* **2009**, *15*, 42–44; c) D.-W. Yoon, D. E. Gross, V. M. Lynch, C.-H. Lee, P. C. Bennett, J. L. Sessler, *Chem. Commun.* **2009**, 1109–1111; d) R. Nishiyabu, M. A. Palacios, W. Dehaen, P. Anzenbacher, Jr., *J. Am. Chem. Soc.* **2006**, *128*, 11496–11504; e) M. S. Vickers, K. S. Martindale, P. D. Beer, *J. Mater. Chem.* **2005**, *15*, 2784–2790.
[10] For selected examples, see: a) X. C. Jiang, A. B. Yu, *Langmuir* **2008**, *24*, 4300–4309; b) V. Amendola, E. Bastianello, L. Fabbrizzi, C. Mangano, P. Pallavicini, A. Perotti, A. M. Lanfredi, F. Ugozzoli, *Angew. Chem.* **2000**, *112*, 3039–3042; *Angew. Chem. Int. Ed.* **2000**, *39*, 2917–2920; c) W. Goodall, J. A. G. Williams, *J. Chem. Soc. Dalton Trans.* **2000**, 2893–2895; d) D. Parker, K. Senanayake, J. A. G. Williams, *Chem. Commun.* **1997**, 1777.
[11] F. Wang, H. Chen, S. Parsons, I. D. H. Oswald, J. E. Davidson, P. J. Sadler, *Chem. Eur. J.* **2003**, *9*, 5810–5820.
[12] Aqueous solutions of complex **1a** can be stored in air for weeks without noticeable decomposition. For a discussion of Cp*Rh-based chemosensors, see: K. Severin, *Chem. Commun.* **2006**, 3859–3867.
[13] L. L. Stookey, *Anal. Chem.* **1970**, *42*, 779–781. In the original report, IR spectroscopy was used to infer *para* substitution for the two sulfonate groups. For samples purchased from Sigma–Aldrich or Acros Organics, however, we have ^{1}H NMR spectroscopic and crystallographic evidence to suggest that the sulfonate groups are, in fact, located in the *meta* positions on the phenyl rings.
[14] a) A. Nutton, P. M. Bailey, P. M. Maitlis, *J. Chem. Soc. Dalton Trans.* **1981**, 1997–2002; b) J. W. Kang, P. M. Maitlis, *J. Organomet. Chem.* **1971**, *30*, 127–133.
[15] M. Staffilani, K. S. B. Hancock, J. W. Steed, K. T. Holman, J. L. Atwood, R. K. Juneja, R. S. Burkhalter, *J. Am. Chem. Soc.* **1997**, *119*, 6324–6335.
[16] a) T. Dwars, E. Paetzold, G. Oehme, *Angew. Chem.* **2005**, *117*, 7338–7364; *Angew. Chem. Int. Ed.* **2005**, *44*, 7174–7199; *Angew. Chem.* **2005**, *117*, 7338–7364; b) J. H. Fendler, E. J. Fendler in *Catalysis in Micellar and Macromolecular Systems*, Academic Press, New York, **1975**.
[17] E. Feitosa, M. R. S. Brazolin, R. M. Z. G. Naal, M. P. F. De M. Del Lama, J. R. Lopes, W. Loh, M. Vasilescu, *J. Colloid Interface Sci.* **2006**, *299*, 883–889.
[18] J. L. Beltrán, M. D. Prat, R. Codony, *Talanta* **1995**, *42*, 1989–1997.
[19] A. Safavi, H. Abdollahi, *Microchem. J.* **2001**, *69*, 167–175.
[20] a) R. Barnados-Rodríguez, J. Estelrich, *J. Phys. Chem. B* **2009**, *113*, 1972–1982; b) H. Rosenbluth, B. Weiss-Lopez, A. F. Olea, *Photochem. Photobiol.* **1997**, *66*, 802–809.
[21] D. Roy, R. Karmakar, S. K. Mondal, K. Sahu, K. Bhattacharyya, *Chem. Phys. Lett.* **2004**, *383–400*, 147–151.
[22] a) J. R. Lacowicz in *Principles of Fluorescence Spectroscopy*, 3rd ed., Plenum Press, New York, **2006**; b) E. Blatt, R. C. Chatelier, W. H. Sawyer, *Biophys. J.* **1986**, *50*, 349–356.
[23] a) S. Gamsey, A Miller, M. M. Olmstead, C. M. Beavers, L. C. Hirayama, S. Pradhan, R. A. Wessling, B. Singaram, *J. Am. Chem. Soc.* **2007**, *129*, 1278–1286; b) S. Gamsey, N. A. Baxter, Z. Sharrett, D. B. Cordes, M. M. Olmstead, R. A. Wessling, B. Singaram, *Tetrahedron* **2006**, *62*, 6321–6331; c) D. B. Cordes, S. Gamsey, Z. Sharrett, A. Miller, P. Thoniyot, R. A. Wessling, B. Singaram, *Langmuir* **2005**, *21*, 6540–6547; d) E. Pino, A. M. Campos, E. Lissi, *J. Photochem. Photobiol. A* **2003**, *155*, 62–68; e) C. Prayer, T.-H. Tran-Thi, S. Pommeret, P. d'Oliveira, P. Meynadier, *Chem. Phys. Lett.* **2000**, *323*, 467–473; f) E. B. de Borba, C. L. C. Amaral, M. J. Politi, R. Villalobos, M. S. Baptista, *Langmuir* **2000**, *16*, 5900–5907.
[24] T. F. Hunter, *Chem. Phys. Lett.* **1980**, *75*, 152–155.
[25] a) D. P. Smith, E. Kohen, M. F. Maestre, R. H. Fish, *Inorg. Chem.* **1993**, *32*, 4119–4122; b) A. Buryak, A. Pozdnoukhov, K. Severin, *Chem. Commun.* **2007**, 2366–2368; c) A. Buryak, F. Zaubitzer, A. Pozdnoukhov, K. Severin, *J. Am. Chem. Soc.* **2008**, *130*, 11260–11261.
[26] L. Dadci, H. Elias, U. Frey, A. Hörnig, U. Koelle, A. E. Merbach, H. Paulus, J. S. Schneider, *Inorg. Chem.* **1995**, *34*, 306–315.
[27] The detection limit was assumed to be $3\sigma_{blank}$ (σ is the standard deviation), see: J. C. Miller, J. N. Miller in *Statistics for Analytical Chemistry*, Ellis Horwood Limited, Chichester, **1984**, pp. 96–100.
[28] Listed on the bottle. For the local tap water sample, we consulted the official website of the city of Lausanne (http://www.lausanne.ch).

Received: May 12, 2010
Published online: June 22, 2010

